Thermodynamics of two lattice ice models in three dimensions

Chizuru Muguruma,[1,2] Yuko Okamoto,[3] and Bernd A. Berg[4,5,*]
[1]*School of International Liberal Studies, Chukyo University, Toyota, Aichi 470-0393, Japan*
[2]*Department of Scientific Computing, Florida State University, Tallahassee, Florida 32306-4120, USA*
[3]*Department of Physics, Nagoya University, Nagoya, Aichi 464-8602, Japan*
[4]*Department of Physics, Florida State University, Tallahassee, Florida 32306-4350, USA*
[5]*Institut für Theoretische Physik und Naturwissenschaflich-Theoretisches Zentrum (NTZ), Universität Leipzig, D-04009 Leipzig, Germany*

(Received 4 June 2008; published 13 October 2008; publisher error corrected 14 October 2008)

In a recent paper we introduced two Potts-like models in three dimensions, which share the following properties: (A) One of the ice rules is always fulfilled (in particular also at infinite temperature, $\beta=0$). (B) Both ice rules hold for ground-state configurations. This allowed for an efficient calculation of the residual entropy of ice I (ordinary ice) by means of multicanonical simulations. Here we present the thermodynamics of these models in more details. Despite their similarities with Potts models, no sign of a disorder-order phase transition is found.

DOI: 10.1103/PhysRevE.78.041113 PACS number(s): 05.50.+q, 11.15.Ha, 12.38.Gc, 25.75.−q

I. INTRODUCTION

By experimental discovery [1] it was found that ice I (ordinary ice) has in the zero temperature limit a residual entropy $S/N=k\ln(W_1)>0$, where N is the number of molecules and W_1 the number of configurations per molecule. Subsequently Pauling [2] based the estimate $W_1^{\text{Pauling}}=3/2$ on the ice rules:

(1) There is one hydrogen atom on each bond (then called hydrogen bond).

(2) There are two hydrogen atoms near each oxygen atom (these three atoms constitute a water molecule).

Pauling's combinatorial estimate turned out to be in excellent agreement with subsequent refined experimental measurements [3]. This may be a reason why it took 25 years until Onsager and Dupuis [4] pointed out that $W_1=1.5$ is only a lower bound. Subsequently Nagle [5] used a series expansion method to derive the estimate $W_1^{\text{Nagle}}=1.506\,85(15)$.

In [6] we introduced two combinatorial models with nearest-neighbor interactions on three-dimensional (3D) hexagonal lattices, a 6-state ($6s$) H_2O molecule model and a 2-state ($2s$) hydrogen bond model. In these models one can calculate the residual entropy of ice I by means of multicanonical (MUCA) [7–9] simulations with high precision. Our estimate $W_1^{\text{MUCA}}=1.507\,38(16)$ is in reasonably good agreement with Nagle's result. In [10] these calculations were extended to partially ordered ice for which previously only entropy estimates along Pauling's heuristic arguments were available [11,12]. Although these numbers are of direct relevance for real ice, experimental estimates [13–16] are unfortunately not accurate enough to be sensitive to the corrections of Pauling-like estimates.

In this paper we investigate the thermodynamics of our combinatorial models in more details. There exists extensive literature on ice models [17–30]. As discussed in the next section, our $6s$ model can be mapped on the brick ice of [20] and our $2s$ model is closely related to spin ice [23], a geometrically frustrated [31] system for which, similarly as for ice, experimental measurements of ground-states entropies exist [26,27,30], which are (within rather large experimental error bars) in agreement with the combinatorial estimates.

Our two models share with certain spin models [32] that the residual entropy of their ground-states violates the third law of thermodynamics. For real physical systems that is not supposed to be the case [2]. The different proton arrangements are then no longer exactly degenerate in energy, resulting in a proton ordered phase at very low temperatures [33–35].

Superficially our models are similar to q-state Potts models [36] with $q=6$ for the $6s$ and the Ising case $q=2$ for the $2s$ model, which have first ($q=6$) and second ($q=2$) order phase transitions in two dimensions (2D) as well as in three dimensions (3D). Therefore, one might expect that in the crude approximation of our models the water-ice transition is

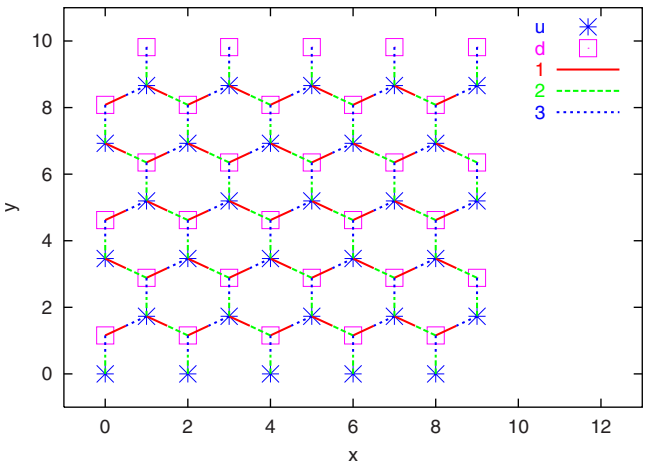

FIG. 1. (Color online) Lattice structure of one layer of ice I (reproduced from Ref. [6]). The up (u) sites are at $z=1/\sqrt{24}$ and the down (d) sites at $z=-1/\sqrt{24}$. Three of its four pointers to nearest-neighbor sites are shown.

*Corresponding author.

reflected by a disorder-order transition similar to that of Potts models. In this paper we provide numerical evidence that this is not the case. Down to their ground-state configurations our models show no sign of a phase transition.

In detail our models are introduced in the next section and our numerical results are presented in Sec. III. Summary and conclusions follow in Sec. IV.

II. MODELS

Our models are defined on hexagonal lattices with a structure as depicted in Fig. 1 [37]. In $6s$ H_2O molecule model, ice rule (2) is always enforced. At each oxygen atom there are precisely two hydrogens atoms close and we allow for six distinct orientations of each H_2O molecule. Its energy is defined by

$$E = -\sum_b h(b, s_b^1, s_b^2). \tag{1}$$

Here, the sum is over all bonds b of the lattice (s_b^1 and s_b^2 indicate the dependence on the states of the two H_2O molecules, which are connected by the bond) and

$$h(b, s_b^1, s_b^2) = \begin{cases} 1 & \text{for a hydrogen bond,} \\ 0 & \text{otherwise.} \end{cases} \tag{2}$$

In the $2s$ H-bond model, ice rule (1) is always enforced and we allow for two positions of each hydrogen nucleus on a bond. The energy is defined by

$$E = -\sum_s f(s, b_s^1, b_s^2, b_s^3, b_s^4), \tag{3}$$

where the sum is over all sites (oxygen atoms) s of the lattice, $(s, b_s^1, b_s^2, b_s^3, b_s^4)$ indicate the dependence on the four bonds which emerge from site s and the function $f(s, b_s^1, b_s^2, b_s^3, b_s^4)$ is given by

$$f(s, b_s^1, b_s^2, b_s^3, b_s^4) = \begin{cases} 2 & \text{for two hydrogen nuclei close to } s, \\ 1 & \text{for one or three hydrogen nuclei close to } s, \\ 0 & \text{for zero or four hydrogen nuclei close to } s. \end{cases} \tag{4}$$

The ground-states of either model fulfill both ice rules.

We use units with $k=1$ for the Boltzmann constant, i.e., $\beta = 1/T$. At $\beta=0$ the number of configurations is 6^N for the $6s$ model and 2^{2N} for the $2s$ model. The triviality of our ice models at $\beta=0$ allows one to set the normalization for the entropy and free energy, which can then be connected by a MUCA simulation of the type [8] to β values large enough so that ground-states get sampled.

The gound-state entropy of 2D square ice was rigorously derived by Lieb [17] to be $W_1^{\text{square ice}} = (4/3)^{3/2} = 1.539\,60\ldots$, somewhat larger than that of real ice. Krausche and Nadler introduced a nonzero temperature extension of Lieb's model and a 3D version, they called brick ice [20], which can be mapped on our $6s$ model (due to use of a cubic lattice their coordinates are different, but only the topology matters, which turns out to be identical to ours).

In spin ice with an Ising anisotropy [23] the two positions of the hydrogen in our $2s$ model are replaced by up-down spins σ_l at the center of the link, constituting a frustrated [31] spin model. The configurations of our $2s$ model and Ising spin ice are then in one to one correspondence, while the energy functions are slightly different. Assuming $\sigma_l = \pm 1$ and $J_{lk} = -1$ connection between spins, one gets instead of our Eq. (4) for spin ice

$$f_{\text{spin ice}}(s, \sigma_s^1, \sigma_s^2, \sigma_s^3, \sigma_s^4) = \begin{cases} 2 & \text{for two spins up and two spins down,} \\ 0 & \text{for one spin up and three spins down,} \\ 0 & \text{for one spin down and three spins up,} \\ -6 & \text{for either all spins up or all spins down,} \end{cases} \tag{5}$$

where $(s, \sigma_s^1, \sigma_s^2, \sigma_s^3, \sigma_s^4)$ denotes now the dependence on the four spins of the tetrahedra at site s. Obviously this changes the temperature dependence of observables like energy and specific heat, but has no bearing on the ground-state entropy or the existence of a phase transition.

As the $q=6$ Potts model our $6s$ model has six elementary states per site (the allowed orientations of the molecule), while the $2s$ model has two states per link like the $q=2$ Ising case. For the $2s$ model the Ising symmetry (most clearly as $\sigma_l \to -\sigma_l$ in the spin ice interpretation) is also obvious. This symmetry can be broken by applying a magnetic field [26] or, as done in [10], by introducing an overlap with one ground-state reference configuration.

TABLE I. Overview of our multicanonical simulations. Here, n_x, n_y, n_z are the number of lattice sites along the x, y, z axes, and $N=n_x n_y n_z$.

n_x	n_y	n_z	N	cycles ($6s$)	cycles ($2s$)
4	8	4	128	37828	141825
4	12	6	288	9455	33205
5	12	6	360	4891	21621
6	12	8	576	653	11479
7	16	8	896	412	6452
8	20	10	1600	215	1587
10	24	12	2880	1133	506

III. SIMULATION RESULTS

Using periodic boundary conditions (BCs), our simulations are based on a lattice construction [38] similar to that set up for Potts models in [9]. The lattice sizes used are compiled in Table I. The lattice contains then $N=n_x n_y n_z$ sites, where n_x, n_y, and n_z are the number of sites along the x, y, and z axes, respectively. Periodic BCs restrict the allowed values of n_x, n_y, and n_z to $n_x=1,2,3,\ldots$, $n_y=4,8,12,\ldots$, and $n_z=2,4,6,\ldots$. Otherwise the geometry does not close properly.

As proposed in [39] we employed a Wang-Landau [40] recursion for determining the MUCA weights and performed subsequent MUCA data production with fixed weights. With one exception we used $32\times(20\times10^6)$ sweeps per lattice for data production. For the largest lattice of the $6s$ model we produced a 10 times larger statistics. Table I lists for each lattice size and model the number of cycling events from the average disordered energy E_0 at $\beta=0$ to the ground-state energy E_g and back,

$$E_0 \leftrightarrow E_g, \tag{6}$$

as recorded during the production part of the run. From the energy functions (1) and (3) one finds $E_0=-N$ for the $6s$ model (there are two hydrogen atoms per oxygen and the probability to form a hydrogen bond is $1/2$), $E_0=-1.25N$ for the $2s$ model (at one site there are 16 arrangements of hydrogen atoms with average energy contribution $-[2\times0+8\times1+6\times2]/16=-1.25$), and $E_g=-2N$ for both models. In the following we restrict the β range of our figures to $0\leqslant\beta\leqslant5$, which is large enough to sample ground-states in sufficient numbers so that extrapolations down to temperature $T=0$ become controlled.

In Fig. 2 we show the average energy per site, E/N, from the MUCA simulations of our two models as obtained by the reweighting procedure [9] (note that we use E for the energy of configuration as well as for average values over configuration energies and assume the reader knows to distinguish them). Obviously there are almost no finite-size effects, because the curves from all lattice sizes fall within small statistical errors, which are not visible on the scale of this figure, on top of one another.

The specific heat per site, C/N, is calculated via the fluctuation-dissipation theorem,

$$C=\frac{dE}{dT}=-\beta^2\frac{dE}{d\beta}=\beta^2(\langle E^2\rangle-\langle E\rangle^2), \tag{7}$$

and plotted in Fig. 3. Finite-size corrections are now visible for the smallest, $N=128$ and $N=288$, lattices. For the other lattices the curves fall again within error bars on top of one another. Error bars were calculated with respect to 32 jackknife bins and are at some β values included for our largest, $N=2880$, lattice. Some data for these points are given in Table II. Fluctuations increase with lattice size, so that it is more difficult to obtain accurate results on large lattices than on small ones. Note that the $N=2880$ data for the $6s$ model rely on a 10 times larger statistics than those for the $2s$ model, while the error bars are only slightly smaller. As noticed before [6], the simulations of the $2s$ model are more efficient for determining the ground-state entropy than simulations of the $6s$ model.

We want to contrast Fig. 3 with specific heat results for the 6-state and 2-state Potts models on L^D lattices. Immediately, one notices that it is not entirely clear whether this comparison should be done in 2D or 3D. While the space dimension in which our ice models are embedded is clearly 3D, each site is connected through links with four neighboring sites, which is the Potts model situation in 2D. The 2D and 3D Ising models are well known for their second-order

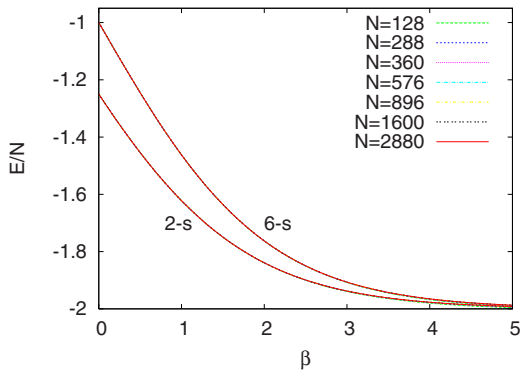

FIG. 2. (Color online) Energy per site for the $6s$ and $2s$ models. On the scale of this figure the curves for different lattice sizes fall on top of one another.

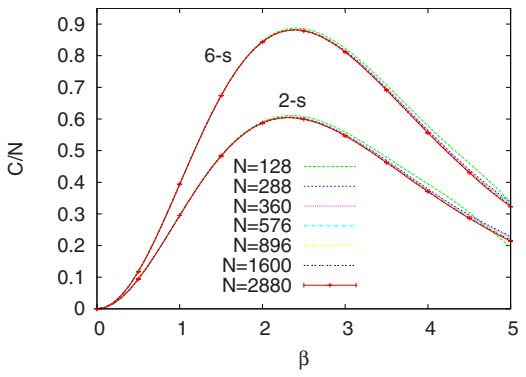

FIG. 3. (Color online) Specific heat per site for the $6s$ and $2s$ models. For $N>288$ the curves fall on top of one another on the scale for this figure.

TABLE II. Some specific heat data C/N with error bars (in parentheses) for the $N=2880$ lattice.

β	$6s$ model	$2s$ model
0.5	0.1175119(77)	0.093780(17)
1.5	0.673681(71)	0.48331(11)
2.5	0.87873(19)	0.59913(22)
3.5	0.69110(35)	0.46235(42)
4.5	0.43066(45)	0.28637(61)

phase transitions. The specific heat is logarithmically divergent in 2D [41] and has a critical exponent $\alpha \approx 0.1$ in 3D (see [42] for a review). The 2D and 3D 6-state Potts models have first-order transitions with a larger latent heat per spin in 3D than in 2D (in the normalization of [9] $\Delta E/N = 0.402\,928\,28$ in 2D [43] and $\Delta E/N = 2.364\,42 \pm 0.000\,17$ in 3D [44]).

For second-order transitions the maximum of the specific heat diverges $\sim \ln(L)$ for a logarithmic divergence ($\alpha=0$) and $\sim L^{\alpha/\nu}$ for $\alpha>0$, where ν is the critical exponent of the correlation length. In case of first-order phase transitions the peak in the specific heat diverges $\sim L^D$, where the proportionality factor is [45] $(\beta_t)^2(\Delta E/N)^2$ with β_t the inverse transition temperature and $\Delta E/N$ the latent heat per spin.

In Figs. 4 and 5 we plot the specific heat on various lattices for the two extremes, the weak logarithmic divergence for the 2D Ising model and the strong divergence for the 3D 6-state Potts model. For the 2D Ising model the analytical solutions of Ferdinand and Fisher [46] are plotted, while the plots for the 3D 6-state Potts model rely on recent numerical results [44]. It is clear that even the case of a weak logarithmic divergence is markedly distinct from the behaviors in Fig. 3, where no finite-size effects are observed within the rather accurate statistical errors. This distinction becomes all too obvious when the comparison is made with the strong first-order phase transition of the 3D 6-state Potts model.

In contrast to the Potts model, the ground-state symmetry of the two ice models is not broken at a finite value of β. As emphasized in [19,20] the specific heat in ice shows some similarity to that of the 1D Ising model. For the 1D Ising model the low dimension prevents symmetry breaking at finite values of β. The energy barrier between the all spins up

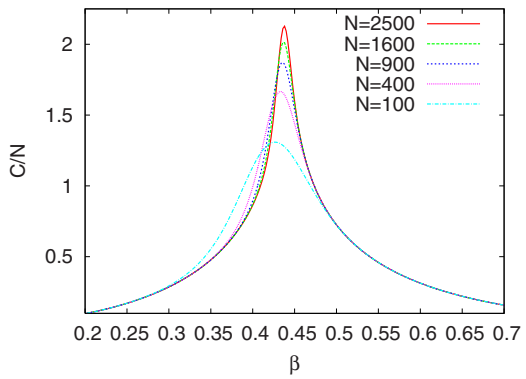

FIG. 4. (Color online) Specific heat per site for the 2D Ising model on $N=L^2$ lattices.

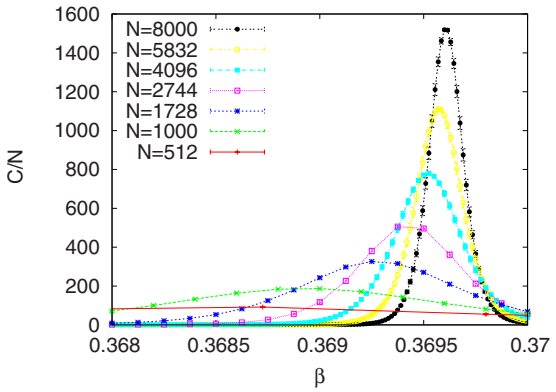

FIG. 5. (Color online) Specific heat per site for the 3D 6-state Potts model on $N=L^3$ lattices.

versus down state stays finite in the infinite volume limit: Flipping the orientations of the spins sequentially, just two links are frustrated on any periodic lattice. Thus the $s_i \to -s_i$ symmetry is preserved.

Similarly barriers between our ice model ground-states stay finite, though the reason lies no longer in the low space dimension, but in the existence of a nonzero ground-state entropy and a corresponding ground-state ensemble. The finiteness of the barriers follows then from the hydrogen-bonded loop algorithm of Rahman and Stillinger [47], which was used and further developed in [18,21,24,48]. This algorithm finds first a closed loop of hydrogen bonds and generates in a second step new hydrogen positions by shifting all hydrogens to the other side of their bond. Ergodicity in the ensemble of ground-states has been demonstrated in Refs. [21,24]. Performing the reassignments of hydrogen positions along a path sequentially, it is obvious that for our energy functions (1) and (3) the encountered energy changes stay finite: For the $6s$ model ice rule (2) and for the $2s$ model ice rule (1) is never violated for more than three molecules.

To complete the picture of our two ice models we plot in Figs. 6 and 7 their free energy and entropy densities as obtained from our simulations, using as input the known normalizations at $\beta=0$. In the cases at hand these are $S_0/N = \ln(6)$ for the $6s$ and $S_0/N=\ln(4)$ for the $2s$ model. Relative statistical errors are smaller than those in Fig. 3 for the specific heat. In the $\beta \to \infty$ limit our data improve slightly on the results reported in Ref. [6], because we have with $N=2880$ one larger lattice added. Consistent fits to the previously discussed form $W_1(x) = W_1^{\mathrm{MUCA}} + a_1 x^\theta$, $x = 1/N$ combine to

$$W_1^{\mathrm{MUCA}} = 1.507\,21(13) \quad \text{and} \quad \theta = 0.901(16). \tag{8}$$

The error bars in parentheses are purely statistical and do not reflect eventual, additional systematic errors due to higher-order finite-size corrections. Note that we did not investigate bond statistics in the ground-state ensemble, which one may expect to exhibit critical correlations.

IV. SUMMARY AND CONCLUSIONS

The unusual properties of water and ice owe their existence to a combination of strong directional polar interac-

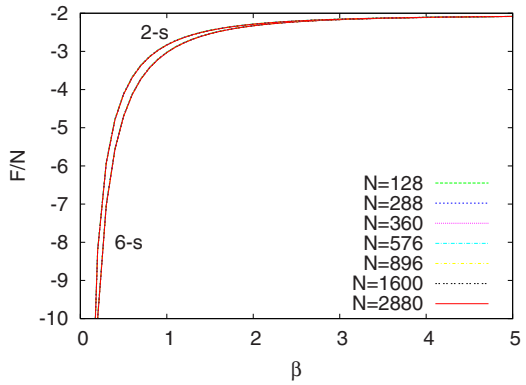

FIG. 6. (Color online) Free energy.

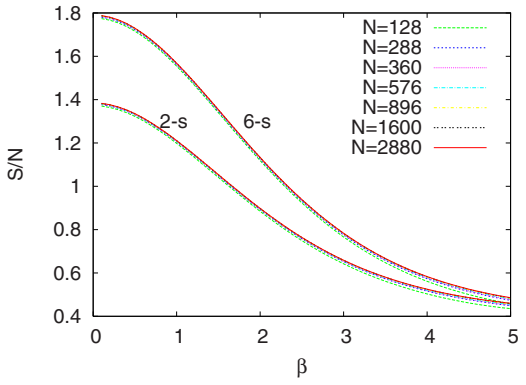

FIG. 7. (Color online) Entropy.

tions and a network of specifically arranged hydrogen bonds [49–51]. The ground-state structure of such a network can be described by simple lattice models, which are defined by the energy functions (1) and (3).

In the present paper we have presented finite-size scaling evidence that there is no phase transition at finite β in these models. This makes reliable MUCA estimates of the combinatorial ground-state entropy of ice I particularly easy. The reason for the lack of a transition appears to lie in the large ground-state entropy, $S/N=\ln(W_1)$, of these models (violating the third law of thermodynamics) together with the fact that the barriers between the ground-states stay finite in the infinite volume limit. Apparently similar results are found for some other geometrically frustrated spin systems, for instance the 2D Villain model [52,53].

Beyond this paper, one may now address the question about the physical origin of the ice-water-ice transition by extending our investigation along the following lines, monitoring each case for the occurrence of a phase transition.

(1) Extend the 6*s* model to continuous rotations of Euler angles with nearest neighbor interaction of the molecules based on one of the TIP4P-like water energies [54], keeping the center of mass (or the oxygen) of each molecule fixed.

(2) Add the non-local interaction between these molecules, still allowing only rotational degrees of freedom.

(3) Add translational degrees of freedom.

ACKNOWLEDGMENTS

We thank Santosh Dubey for providing the plot of Fig. 5. Partial support for this work was received for B.B. from the JSPS and the Humboldt Foundation, for C.M. by the Chukyo University Research Fund, and for Y.O. by the Ministry of Education, Culture, Sports, Science and Technology of Japan, Grants-in-Aid for the Next Generation Super Computing Project, Nanoscience Program and for Scientific Research in Priority Areas, Molecular Theory for Real Systems. B.B. acknowledges useful discussions with Wolfhard Janke.

[1] W. F. Giauque and M. Ashley, Phys. Rev. **43**, 81 (1933).
[2] L. Pauling, J. Am. Chem. Soc. **57**, 2680 (1935).
[3] W. F. Giauque and J. W. Stout, J. Am. Chem. Soc. **58**, 1144 (1936); **58**, 1144 (1936).
[4] L. Onsager and M. Dupuis, Rend. Sc. Int. Fis. Enrico Fermi **10**, 294 (1960).
[5] J. F. Nagle, J. Math. Phys. **7**, 1484 (1966).
[6] B. A. Berg, C. Muguruma, and Y. Okamoto, Phys. Rev. B **75**, 092202 (2007).
[7] B. A. Berg and T. Neuhaus, Phys. Rev. Lett. **68**, 9 (1992).
[8] B. A. Berg and T. Celik, Phys. Rev. Lett. **69**, 2292 (1992).
[9] B. A. Berg, *Markov Chain Monte Carlo Simulations and Their Statistical Analysis* (World Scientific, Singapore, 2004).
[10] B. A. Berg and W. Yang, J. Chem. Phys. **127**, 224502 (2007).
[11] R. Howe and R. W. Whitworth, J. Chem. Phys. **86**, 6443 (1987).
[12] L. G. MacDowel, E. Sanz, C. Vega, and J. L. F. Abascal, J. Chem. Phys. **121**, 10145 (2004).
[13] S. J. La Placa, W. C. Hamilton, B. Kamb, and A. Prakash, J. Chem. Phys. **58**, 567 (1973).
[14] O. Haida, T. Matsuo, H. Suga, and S. Seki, J. Chem. Thermodyn. **6**, 815 (1995).
[15] J. D. Londono, W. F. Kuhs, and J. L. Finney, J. Chem. Phys. **98**, 4878 (1993).
[16] J. D. Lobban, J. L. Finney, and W. F. Kuhs, J. Chem. Phys. **112**, 7169 (2000).
[17] E. H. Lieb, Phys. Rev. **162**, 162 (1967).
[18] A. Yanagawa and J. F. Nagle, Chem. Phys. **43**, 329 (1979).
[19] W. Nadler and T. Krausche, Phys. Rev. A **44**, R7888 (1991).
[20] T. Krausche and W. Nadler, Z. Phys. B: Condens. Matter **86**, 433 (1992).
[21] G. T. Barkema and J. de Boer, J. Chem. Phys. **101**, 6141 (1993).
[22] J. F. Nagle, J. Stat. Phys. **78**, 549 (1995).
[23] M. J. Harris, S. T. Bramwell, D. F. McMorrow, T. Zeiske, and K. W. Godfrey, Phys. Rev. Lett. **79**, 2554 (1997).
[24] G. T. Barkema and M. E. J. Newman, Phys. Rev. E **57**, 1155 (1998).
[25] G. I. Watson, J. Stat. Phys. **94**, 1045 (1999).
[26] A. P. Ramirez, A. Hayashi, R. J. Cava, R. Siddarthan, and B. S.

Shasty, Nature (London) **399**, 333 (1999).
[27] A. P. Ramirez, C. L. Broholm, R. J. Cava, and G. R. Kowach, Physica B **280**, 290 (2000).
[28] S. V. Lishchuk, T. V. Lokotosh, and N. P. Malomuzh, J. Chem. Phys. **122**, 244504 (2005).
[29] M. Girardi and W. Figueiredo, J. Chem. Phys. **125**, 094508 (2006).
[30] G. C. Lau, R. S. Freitas, B. G. Ueland, B. D. Muegge, E. L. Duncan, P. Schiffer, and R. J. Cava, Nat. Phys. **2**, 249 (2006).
[31] A. P. Ramirez, Annu. Rev. Mater. Sci. **24**, 453 (1994).
[32] Y. Chow and F. Y. Wu, Phys. Rev. B **36**, 285 (1987).
[33] N. Bjerrum, Science **115**, 385 (1952).
[34] K. S. Pitzer and J. Polissar, J. Phys. Chem. **60**, 1140 (1956).
[35] S. W. Rick, J. Chem. Phys. **122**, 094504 (2005).
[36] F. Y. Wu, Rev. Mod. Phys. **54**, 235 (1982).
[37] The physical distances in the figure do not matter in the present context. The interested reader can find them explained in [6].
[38] B. A. Berg (unpublished).
[39] B. A. Berg, Comput. Phys. Commun. **153**, 397 (2003).
[40] F. Wang and D. P. Landau, Phys. Rev. Lett. **86**, 2050 (2001).
[41] L. Onsager, Phys. Rev. **65**, 117 (1944).
[42] A. Pelissetto and E. Vicari, Phys. Rep. **368**, 549 (2002).
[43] R. J. Baxter, J. Phys. C **6**, L445 (1973).
[44] A. Bazavov, B. A. Berg, and S. Dubey, Nucl. Phys. B **802**, 421 (2008).
[45] M. S. S. Challa, D. P. Landau, and K. Binder, Phys. Rev. B **34**, 1841 (1986).
[46] A. E. Ferdinand and M. Fisher, Phys. Rev. **185**, 832 (1969).
[47] A. Rahman and F. H. Stillinger, J. Chem. Phys. **57**, 4009 (1972).
[48] S. W. Rick and A. D. J. Haymet, J. Chem. Phys. **118**, 9291 (2003).
[49] J. D. Bernal and R. H. Fowler, J. Chem. Phys. **1**, 515 (1933).
[50] D. Eisenberg and W. Kauzmann, *The Structure and Properties of Water* (Oxford University Press, Oxford 1969).
[51] V. F. Petrenko and R. W. Whitworth, *Physics of Ice* (Oxford University Press, Oxford 1999).
[52] J. Villain, J. Phys. C **10**, 1717 (1977).
[53] J. Lukic, E. Marinari, and O. C. Martin, Europhys. Lett. **73**, 779 (2006).
[54] W. L. Jorgensen, J. Chandrasekhar, J. D. Madra, R. W. Impey, and M. L. Klein, J. Chem. Phys. **79**, 926 (1983).